ARTICLE
Journal of Cellular Biochemistry 114:1498–1509 (2013)

Journal of Cellular Biochemistry

HDAC Inhibitor DWP0016 Activates p53 Transcription and Acetylation to Inhibit Cell Growth in U251 Glioblastoma Cells

Hui Jin, Lei Liang, Lifeng Liu, Weiping Deng,** and Jianwen Liu*

State Key Laboratory of Bioreactor Engineering and Shanghai Key Laboratory of New Drug Design, School of Pharmacy, East China University of Science and Technology, Shanghai, People's Republic of China

ABSTRACT

Here we report a hydroacid named DWP0016, which exhibited HDAC inhibition and induced p53 acetylation in U251 glioblastoma cells. DWP0016 effectively inhibited the cell growth of U251 cells and other four carcinoma cell lines but did not affect the normal cells. Cell cycle distribution analysis showed DWP0016 arrested at G_1 phase cell cycle dose-dependently in U251 cells. DWP0016 induced caspase-dependent and independent apoptosis in U251 cells, which was identified by flow cytometry analysis, caspases activity analysis, Western blotting assay, and caspases inhibition. Mechanisms research suggested that DWP0016 activated transcription and acetylation of tumor suppressor p53. DWP0016 regulated p300, CBP, and PCAF to facilitate p53 acetylation at *lys*382 in U251 cells. In addition, activation of p53 by DWP0016 promoted PUMA to catalyze mitochondrial pathway. Besides, siRNA assay indicated p53 was the key gene to induce growth inhibition, cell cycle arrest, and apoptosis in DWP0016 treated U251 cells. Conclusively, our results show DWP0016 is a potent HDAC inhibitor and the anti-tumor activity is consistent with its intended p53 activation mechanisms. These findings indicate the promising antitumor potential of DWP0016 for further glioblastoma treatment applications. J. Cell. Biochem. 114: 1498–1509, 2013.

KEY WORDS: HDAC INHIBITOR; CYCLE ARREST; APOPTOSIS; P53; ACETYL-P53

The tumor suppressor p53 coordinates cell-cycle progression and apoptosis as "the guardian of the genome" [Stegh and DePinho, 2011]. P53 plays an important role in apoptosis, genomic stability, and angiogenesis inhibition [Vousden and Lane, 2007]. Different post-translational modifications affect the function of p53 including acetylation. Previous reports show several transcriptional factors including p300, co-activators p300/CREB-binding protein (CBP) and p300/CBP-associated factor (PCAF) involve in acetylating p53 at lysine site. These transcriptional factors enable p53 activation to induce cell cycle arrest and apoptosis [Guo et al., 2000; Luo et al., 2000; Ito et al., 2001]. Besides, P53 co-acts with different pathways to regulate cell cycle and apoptosis. Mitochondrial pathway including Bcl-2 family is one of the most important pathway [Miyashita and Reed, 1995; Nakano and Vousden, 2001; Jeffers et al., 2003; Hastak et al., 2005]. The Bcl-2 family comprise different proteins with anti-apoptotic genes and pro-apoptotic such as Bcl-2, Bax, Bid, etc. [Adams and Cory, 2007]. PUMA, which is a pro-apoptotic member belonging to Bcl-2 family, scaffold p53 and Bcl-2 family to facilitate cell growth, cell cycle, and apoptosis [Nakano and Vousden, 2001]. These interactions make p53 exerting unique biochemical functions and playing an important role in preventing cancer.

P53 is often mutant or low expressed in glioblastoma [Watanabe et al., 1997]. Glioblastoma is an aggressive and lethal cancer, accounting for most of primary brain tumors in adults with median survival of less than 12 months [Grzmil et al., 2011]. Glioblastoma is characterized by genetic alterations largely, affecting different genes that control cell growth, apoptosis, angiogenesis, and invasion [Nagarajan and Costello, 2009]. Previous studies conclude that dysregulation on p53 is one core reason for the formation of glioblastoma [Stambolic et al., 2001]. These investigations indicate the significant role of p53 for glioblastoma treatment. However, the potential of p53 in glioblastoma treatment still remained largely unknown.

Histone deacetylases (HDAC) modify histone tail through deacetylating amino-terminal lysine residues, which results in

The authors declare that they have no conflict of interest.

Grant sponsor: Shanghai Committee of Science and Technology; Grant numbers: 09JC1404500, 11DZ2260600; Grant sponsor: Shanghai Leading Academic Discipline Project; Grant number: Project No. B507.

*Correspondence to: Prof. Jianwen Liu, East China University of Science and Technology, #268, 130 Meilong Road, 200237 Shanghai, People's Republic of China. E-mail: liujian@ecust.edu.cn

**Correspondence to: Weiping Deng, East China University of Science and Technology, 130 Meilong Road, 200237 Shanghai, People's Republic of China. E-mail: weiping_deng@ecust.edu.cn

Manuscript Received: 26 March 2012; Manuscript Accepted: 18 December 2012

Accepted manuscript online in Wiley Online Library (wileyonlinelibrary.com): 7 January 2013

DOI 10.1002/jcb.24491 • © 2013 Wiley Periodicals, Inc.

chromatin remodeling related to multiple diseases, especially for tumor genesis [Choudhary et al., 2009]. Based on their significance in epigenetic regulation, HDAC are regarded as new verified targets for cancer therapies [Gray and Ekstrm, 2001; Acharya et al., 2005; Baylin and Ohm, 2006]. In recent years, compounds inhibiting HDAC are identified to harbor multiple cellular effects resulting in tumor-cell proliferation inhibition, cell cycle block and apoptosis induction [Baylin and Ohm, 2006]. A serials of HDAC inhibitors (HDACi) enter preclinical and clinical trials, exhibiting predominant anti-tumor effects with an advantage over traditional antitumor agents [Marks et al., 2003a; Egger et al., 2004]. Studies report that HDAC inhibitor Vorinostat (SAHA) sensitizes glioblastoma cells to chemotherapy and radiation in vitro, ex vivo, and in vivo. The efficacy in clinical trials for gliomas with SAHA alone or in combination therapy suggests the therapeutic potential of HDACi on glioblastoma [Eyülpoglu et al., 2005; Kumagai et al., 2007; Ugur et al., 2007]. Documents increasingly appear to demonstrate the mechanisms underlying the anticancer effects of different HDACi, such as regulating various genes, co-acting with cell signal pathways [Chen et al., 2005; Drummond et al., 2005; Bolden et al., 2006]. Nevertheless, new HDAC inhibitors are still in demand and the potential to treat glioblastoma with HDACi remained largely unknown.

In this study, we report a HDAC inhibitor DWP0016 (Fig. 1), which effectively inhibited the proliferation of glioblastoma U251 cells. DWP0016 induced G_1 cell cycle arrest and apoptosis in U251 cells. The molecular mechanism research showed DWP0016 evoked the transcription and acetylation of p53 with p300, CBP, and PCAF involvement. In addition, p53 activation mediated Bax expression and PUMA promotion to dysregulate mitochondrial pathway in U251 cells. In summary, these findings suggest that DWP0016 activated p53 to treat U251 cells, which made DWP0016 becoming a potential therapeutic candidate for glioblastoma treatment.

MATERIALS AND METHODS

CHEMICALS

DWP0016 {(*E*)-3-(2-benzyl-5-(2-(piperidin-1-yl)ethyl)-2,3,4,5-tetrahydro-1*H*-pyrido[4,3-b]indol-8-yl)-*N*-hydroxyacrylamide} was prepared by the synthesis group, via 10 steps with an overall yield of 7% in 98% purity. The structure of DWP0016 was confirmed by the analysis of its ^{1}H NMR, ^{13}C NMR, and MS spectra. A 20 mM stock solution of DWP0016 was prepared with dimethyl sulfoxide (DMSO) and diluted in culture media for all experiments in vitro. The final DMSO concentration was <0.1% (v/v). The controls were treated with the same amount of vehicle. SAHA was purchased from Sigma and Caspase inhibitor Z-VAD was purchased from Promega.

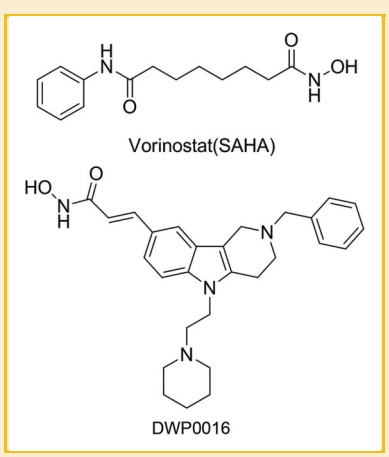

Fig. 1. The structures of DWP0016 and SAHA.

CELL LINES AND CELL CULTURE

Cell lines were purchased from Cell Bank of Type Culture Collection of Chinese Academy of Sciences (Shanghai, China), including: human glioblastoma cell line (U251), human glioblastoma cell line (U-87), human non-small cell lung carcinoma cells (A549), breast carcinoma cell line (MCF-7), human colon carcinoma cells (HCT-116), and human normal liver cell line (L-02). Normal human astrocytes (HA) were obtained from ScienCell (San Diego, CA). A549 and HCT-116 cells were cultured in Roswell Park Memorial Institute (RPMI) 1640 medium supplemented with 10% bovine serum, MCF-7 cells were maintained in Dulbecco's Modified Eagle Medium (DMEM) medium supplemented with 10% calf serum. U251 and U-87 cells were grown in DMEM: F12 (1:1) with 10% fetal calf serum. L-02 cells were cultured in RPMI 1640 medium supplemented with 20% fetal calf serum. HA were cultured in astrocyte medium (ScienCell). Penicillin (100 U/mL) and streptomycin (100 U/mL) were added to all the mediums. Cells were incubated at 37°C in a humidified atmosphere of 95% air and 5% CO_2.

CELL VIABILITY ASSAY

3-(4,5-Dimethylthiazol-2-yl)-2,5-diphenyltetrazolium bromide (MTT, Sigma) assay was performed to assess cell viability with drug exposure as described previously [Fournel et al., 2008]. Briefly, cells in 96-well plates were incubated with DWP0016 at the concentration of 0.156, 0.3125, 0.625, 1.25, 2.5, 5, and 10 μM for 48 h at 37°C. For time extension effects investigations on U251 cells, cells were treated by DWP0016 in the concentration of 0.156, 0.3125, 0.625, 1.25, 2.5, 5, and 10 μM for 12, 24, 36, 48, and 72 h. MTT was added at certain time points and the absorbance values were collected in an Automated Microplate Reader (Multiskan Ex, Finland) at 570 nm using a reference at 630 nm. The values were converted to cell numbers according to a standard growth curve of the relevant cell line. The concentration which reduced cell numbers to 50% relative to DMSO treated cells was calculated as IC_{50} by using a Bliss assay.

INHIBITION OF HDAC ASSAY IN VITRO

The HDAC Fluorimetric Assay Kit (AK-500, Biomol) was used as the producer guided. Briefly, HDAC enzymes were incubated with DWP0016 or SAHA and the reactions were initiated by adding *Fluor-de-Lys* substrate at room temperature. After 45 min, *Fluor-de-Lys* developer was added and the mixture was incubated for another 15 min before reactions stopped. Fluorescence was measured by using a Multi-Mode Microplate Reader (Biotek, US) with excitation at 360 nm and emission at 460 nm. The concentration, which reduced enzymes activity to 50% relative to DMSO treated cells, was determined as IC_{50}. The IC_{50}s were calculated from the dose–

response inhibition curves using nonlinear regression (sigmoidal fit) with Graph Pad Prism (Graph Pad Software, CA).

FLOW CYTOMETRIC ANALYSIS OF CELLULAR DNA CONTENT

The cell distribution analysis was performed as previously reported [Liang et al., 2010]. Cells were incubated with DWP0016 at the concentration of 0.625, 1.25, and 2.5 μM for 48 h. For time extension effects investigations, cells were treated with DWP0016 at the concentration of 1.25 μM for 24, 48, and 72 h. Then both harvested treated and untreated cells were fixed with 70% ice-cold ethanol and kept at −20°C overnight. Fixed cells were centrifuged, washed, and resuspended in PBS containing in concentration of 50 μg/ml of propidium iodide (PI, Sigma) and 100 μg/ml of DNase-free RNase at 37°C before FCM analysis as previously reported [Li et al., 2005]. Cell cycle was analyzed by using cell cytometer (FACScan, Becton Dickinson) and CellQuest Pro software.

FLOW CYTOMETRIC ANALYSIS OF APOPTOSIS AND NECROSIS

Apoptosis and necrosis assessment was performed as previously reported [Liang et al., 2010] by using an Annexin-V/FITC apoptosis detection kit (Invitrogen, USA) by the manufacture's instruction. Briefly, cells were incubated with DWP0016 at the concentration of 0.625, 1.25, and 2.5 μM for 48 h. For time extension effects investigations, cells were treated with DWP0016 at the concentration of 1.25 μM for 24, 48, and 72 h. Harvested cells were stained with Annexin-V/FITC and PI in binding buffer for 15 min at room temperature in the dark. The samples were analyzed by FACScan flow cytometry (Becton Dickinson, USA) to determine the percentage of cells displaying Annexin-V and PI staining. The proportion in the up-left quadrant was defined as the entire necrosis. The up-right and low-right quadrants were defined as late-apoptosis and early-apoptosis.

DETERMINATION OF CASPASE ACTIVITY

The assay was performed as previously reported [Liu et al., 2007]. Cells were treated with DWP0016 at the concentration of 0.625, 1.25, and 2.5 μM for 48 h. After treatment, cells were collected and resuspended in 50 mM Tris–HCl (pH 7.4), 1 mM EDTA, and 10 mM ethyleneglycol-tetraaceticacid (EGTA). Cell lysates were clarified and clear lysates were incubated with 100 μM of enzyme specific colorigenic substrates at 37°C for 1 h. The activity of caspase-3, -8, and -9 was described as the cleavage of colorimetric substrate by measuring the absorbance of 405 nm.

REAL-TIME PCR ANALYSIS

Total RNA was isolated from cells treated with DWP0016 in concentration of 0.625, 1.25, and 2.5 μM by using the RNeasy mini kit (Qiagen, UK) according to the manufacturer's recommendations. Real-time PCR was performed by using SYBR Green Supermix Reverse in Transcription System (Takara, Japan) with 7500 Fast Real-Time PCR System (Applied Biosystems). Primers were synthesized and obtained from Shanghai Sangon Biological Engineering Technology & Services Co, Ltd. (Shanghai, China). The sequences of used primers were: for p53, CGA GAG CTG AAT GAG G (forward) and TGA GTC AGG CCC TTC TGT CT (reverse); for p21, TCC CAA ACG CAA AGA CTG (forward) and AGG GTT TGC GTT TCT GAG (reverse); for cyclin D, AAC TCC CTG CGA AAC ACA C (forward) and TTG AGG GAC GCT TTG TCT G (reverse); for cyclin E, TCT TAC CCT TAC CTA CCT A (forward) and AGA ATG GGA ATG ATG GAT (reverse). Primers for GAPDH as reference gene were GGT CGG AGT CAA CGG ATT TG (forward) and ATG AGC CCC AGC CTT CTC CAT (reverse).

TRANSIENT TRANSFECTION

Cells were transfected with p53 plasmids or specific siRNA by using Lipofectamine^{TM} 2000 Transfection Reagent (Introvigen) according to the manufacturer's instructions as previously reported [Liang et al., 2010]. Briefly, the medium in the cultured cells were moved and the cells were washed with PBS once. Then the PBS solutions with plasmids or siRNA were co-incubated with the cells for another 4 h. Then the cells were collected and analyzed for gene expression. Qualified cells were treated with DWP0016 at the concentrations as indicated before the following analysis. The used wild-type p53 expression vector (pCIneo with full-length p53 cDNA) was constructed as reported previously [Zhu et al., 2001]. P53 siRNA was synthesized by Introvigen and the sequences were 5′-GCA TCT TAT CCG AGT GGA A-3′.

CO-IMMUNOPRECIPITATION (CO-IP)

Co-immunoprecipitation was performed as previously reported [Zhao et al., 2006]. Briefly, treated cells were harvested and then lysed in lysis buffer (1% NP-40, 150 mM NaCl, 50 mM Tris, 0.05% SDS, 1 mM PMSF, and a 1% cocktail of protease inhibitors) on ice for 20 min. Then the cellular lysis was centrifugated at 4°C at 12,000 rpm for 10 min. Specific antibodies were added to the supernatant and co-incubated with the samples for 1 h. Then Agarose G was added to the samples, and the mixed samples were rolled at 4°C for 1 h. After washing the beads, the pellets were dissolved into SDS loading buffer after centrifugation. The protein was analyzed by Western blotting with different antibodies.

WESTERN BLOT ANALYSIS

Cells were treated with DWP0016 at concentration of 0.625, 1.25, and 2.5 μM for 48 h. Protein was abstracted and Western blotting were performed as previously described [Gan et al., 2008]. Briefly, protein were separated in 10–15% SDS–PAGE and transferred to PVDF membrane. After blocked in 5% nonfat milk in TBS-T for 2 h at room temperature, the membrane was incubated with different primary antibodies. The antibodies used in the experiments were: acetylated-H3, p53, $p21^{Waf1/Cip1}$, cyclin D, cyclin E, Bcl-2, Bax, Bid, and β-actin which were obtained from Santa Cruz. Antibodies of cleaved PARP, acetylated-p53 (*lys*382), p300, CBP, PCAF, and PUMA were purchased from Cell Signaling Technology. After extensive washes with TBS-T, the membrane was visualized with BCIP/NBT system and then photographed. The densitometry was analyzed by calculating the relative band OD values of target protein on that of β-actin.

STATISTICAL ANALYSIS

All experiments were conducted in triplicate and repeated at least three times. The results are presented as mean values ± SD. A one-way ANOVA test was used to calculate the statistical significance of

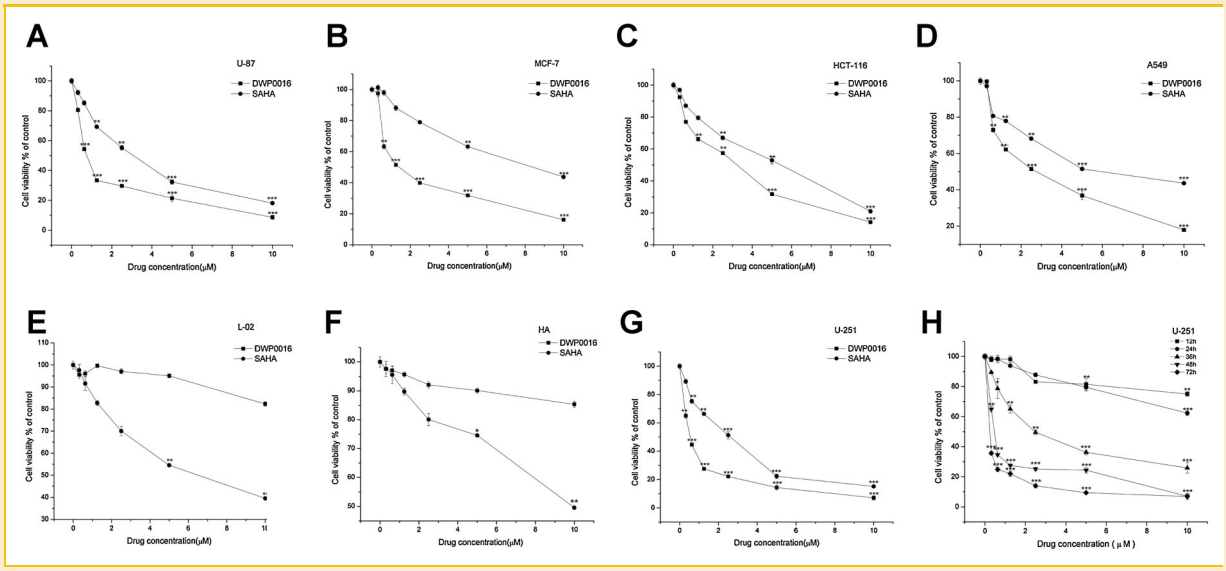

Fig. 2. A. The effects on U-87 cells. B. A. The effects on MCF-7 cells. C. The effects on HCT-118 cells. D. The effects on A549 cells. E. The effects on L-02 cells. F. The effects on Human Astrocytes(HA) cells. G. The effects on U251 cells with different concentrations as indicated. H. The effects on U251 cells with different time exposure as indicated. All experiments were performed at least thrice and independently. Significant differences from untreated control were indicated as $^{*}P < 0.05$; $^{**}P < 0.01$; $^{***}P < 0.001$.

the experimental results. The significance level was set as $^{*}P < 0.05$, $^{**}P < 0.01$, and $^{***}P < 0.001$.

RESULTS

DWP0016 EFFECTIVELY INHIBITED THE GROWTH OF U251 AND OTHER 4 CARCINOMA CELL LINES BUT NOT NORMAL CELLS

MTT assay was performed to test the effects of DWP0016 in different human carcinoma cell lines and normal cells. The results suggested that DWP0016 exhibited remarkably anti-proliferative effects in U-87, U251, HCT-116, A549, and MCF-7 cells dose-dependently (Fig. 2A–D,G). Then we examined the effects on cell growth of U251 at different time points. As shown in Figure 2H, DWP0016 inhibited the proliferation of U251 in a time-dependent manner as indicated. The calculated values in Table I showed that the IC_{50}s of DWP0016 on carcinoma cell lines were much lower than those of SAHA. The IC_{50}s were at least threefold more potent than SAHA in U-87 cells and U251 cells. The lowest IC_{50} was against U251 cells, which indicated the potential of DWP0016 in glioblastma treatment. Importantly, at the response concentrations, DWP0016 did not affect the cell growth of human normal line L-02 nor the HA (Fig. 2E,F). The IC_{50}s on L-02 cells and HA cells were far beyond the responding concentrations on tumor cells and much higher than SAHA. These findings are suggestive that the DWP0016 exhibited potent antitumor potential in glioblastoma without serious toxicity on the normal cells.

DWP0016 INHIBITED HDAC ACTIVITY TO INDUCE HISTONE H3 HYPER-ACETYLATION IN U251 CELLS

We explored the inhibition of HDAC activities and the protein expression of acetylated histone H3 in DWP0016 treated U251 cells. The inhibition on HDAC-1 isotype with DWP0016 exposure was also tested. As shown in Figure 3A, DWP0016 inhibited the activity of HDAC and HDAC-1 dose-dependently. The calculated IC_{50} value of HDAC to DWP0016 exposure was 94 nm, which was close to that of SAHA (65 nm; Fig. 3B). The value of HDAC-1was 26 nm and lower than that to SAHA (37 nm). As results showed in Figure 3C, the protein expression of acetylated histone H3 was much more pronounced in DWP0016 treated cells than that with SAHA treatments. The densitometry results displayed in Figure 3D was also consistent with the protein expression results. These results confirmed the remarkable ability of DWP0016 to inhibit HDAC activity.

TABLE I. IC_{50}s of DWP0016 and SAHA in Various Cultured Cell Lines

Cell lines	U-87	U251	A549	HCT-116	MCF-7	L-02	HA
SA HA	3.09 ± 0.48	2.64 ± 0.39	5.93 ± 0.32	5.44 ± 0.17	8.31 ± 0.35	6.08 ± 0.29	8.49 ± 0.52
DWP 0016	0.77 ± 0.14	0.73 ± 0.17	2.74 ± 0.39	3.38 ± 0.18	1.38 ± 0.25	>10	>10

IC_{50} is the concentration (μmol/L) that reduced cell numbers to 50% relative to DMSO-treated cells. IC_{50}s were determined from experiments at least thrice independently and presented as mean ± SD.

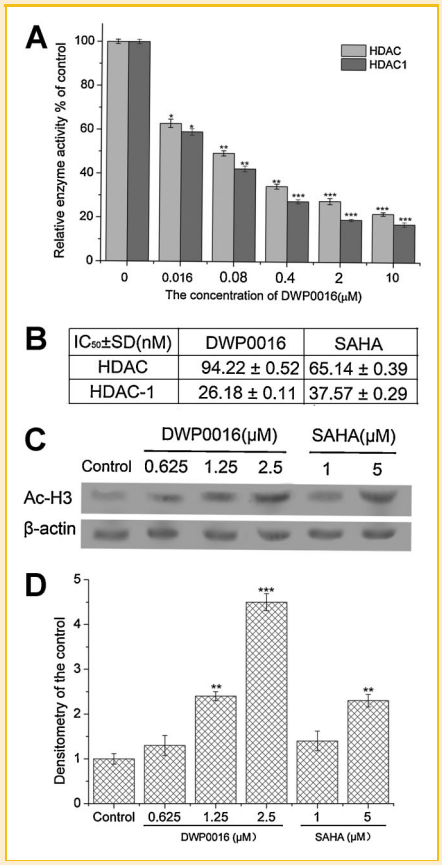

IC_{50}±SD(nM)	DWP0016	SAHA
HDAC	94.22 ± 0.52	65.14 ± 0.39
HDAC-1	26.18 ± 0.11	37.57 ± 0.29

Fig. 3. A: HDAC and HDAC-1 inhibited with DWP0016 and SAHA. The inhibition assays were performed by using Biomol kits with DWP0016 and SAHA diluted in 0.016, 0.08, 0.4, 2, 10 μM. B: IC_{50}s (nmol/L, nM ± SD) of HDAC inhibition with DWP0016 and SAHA. The IC_{50}s were calculated from the dose–response inhibition curves using nonlinear regression (sigmoidal fit) by using Graph Pad Prism (Graph Pad Software, CA). C: Acetylated-histone H3 induced by DWP0016 and SAHA. D: Densitometry analyzed on density of the bands. All in vitro experiments were performed at least thrice and independently. Significant differences from untreated control were indicated as $^{*}P < 0.05$; $^{**}P < 0.01$; $^{***}P < 0.001$.

DWP0016 INDUCED G_1 PHASE CELL CYCLE ARREST IN U251 CELLS DOSE-DEPENDENTLY

As shown in Figure 4A, DWP0016 induced G_1 cell cycle arrest in a dose manner in U251 cells. At the concentration of 0.625 μM, the proportion of gated cells in G_1 phase was 64.05%. Those of 1.25 and 2.5 μM separately were 74.41% and 80.30% in DWP0016 treated U251 cells, which generated statistical significances versus that of control (55.64%; $P < 0.05$; Fig. 4B). The proportion of gated cells in S and G_2 phase depleted with DWP0016 as the concentration accumulation. The proportion of gated cells in G_2 phase was 11.43% with DWP0016 at the concentration of 0.625 μM. Cells arrested in G_2 phase separately were 6.44% and 1.47% by DWP0016 treatment at the concentration of 1.25 and 2.5 μM (Fig. 4B). The G_1 phase arrest was not time-dependent, which indicated other molecular events involved in the mechanisms of DWP0016 when time was extended (data not shown). These data indicated that DWP0016 block at G_1 cell cycle phase in U251 cells dose-dependently.

DWP0016 UPREGUALTED $P21^{CIP/WAF1}$ AND DOWN-REGULATED CYCLIN D AND CYCLIN E AT BOTH MRNA AND PROTEIN LEVEL

We investigated the effects on G_1 cell cycle regulators including $p21^{cip/waf1}$, cyclin D and cyclin E in U251 cells with DWP0016. As shown in Figure 4C, the mRNA level of p21 was promoted to 2.892-fold of the control with DWP0016 at the concentration of 0.625 μM. The mRNA level of p21 rose to 23.278-fold with DWP0016 at the concentration of 2.5 μM. With the exposure of DWP0016 at the concentration of 2.5 μM, the mRNA level of cyclin D decreased to 0.215-fold and that of cyclin E decreased to 0.213-fold of the control. The protein expression of $p21^{cip/waf1}$ was also up-regulated in U251 cells with DWP0016. Correspondingly, the protein expression of cyclin D and cyclin E were relatively down-regulated with DWP0016 dose-dependently as indicated (Fig. 4D). The densitometry results (Fig. 4E) was consistent with the mRNA and protein expression results. These data suggested that the activation of p21 and suppression of cyclin D and cyclin E involved in the cell cycle arrest induced by DWP0016.

DWP0016 INDUCED APOPTOSIS DOSE- AND TIME-DEPENDENTLY IN U251 CELLS BUT NOT U-87 CELLS

We detected the apoptosis in U251 and U-87 cells with DWP0016 by using Annexin V-FITC/PI staining assay. The data suggested that DWP0016 induced apoptotic death in U251 cells dose- and time-dependently (Fig. 5A,B). At the concentration was 0.625 and 1.25 μM, the total apoptosis induced by DWP0016 were 30.1% and 54.75% separately. The total percentage of apoptotic cells was 68.5% with DWP0016 at the concentration up to 2.5 μM which indicated that DWP0016 induced apoptosis in the majority (Fig. 5A). After DWP0016 treatment in the concentration of 1.25 μM for 24 h, the proportion of apoptosis was 31.1% in the U251 cells. When the exposure time prolonged to 48 h, the total apoptosis was significantly promoted to 54.08%. The total apoptosis was elevated to 68.56% after 72 h exposure, which indicated the time-dependent manner of apoptosis by DWP0016. The entire necrosis exhibiting in separate up-left quadrant suggested DWP0016 did not induce apparent necrosis in U251 cells. Interestingly, DWP0016 did not induce apoptosis in U-87 cells (Fig. 5C,D). Neither concentration increase nor time extension with DWP0016 affected the apoptosis proportion in U-87 cells. The total apoptosis in DWP0016 treated U-87 cells made no statistical difference to the control ($P > 0.05$). These data suggested that DWP0016 induced apoptosis in U251 cells but not U-87 cells.

DWP0016 ACTIVATED CASPASES-DEPENDENT AND INDEPENDENT APOPTOSIS IN U251 CELLS

To study whether caspases family involved in the apoptosis, we analyzed the activity of caspase-3, -8, and -9. As shown in Figure 5E, we found the activity of caspase-3, -9 were up-regulated with DWP0016 dose-dependently, and that of caspase-8 was not affected. The activity of caspase-3 was up-regulated to 121.09% compared to control with DWP0016 at the concentration of 0.625 μM. When the concentration rose to 2.5 μM, the activity of caspase-3 was promoted to 284.48% compared to control with DWP0016 exposure. The activity of caspase-9 was activated in a dose-dependent manner with DWP0016 treatment like the up-

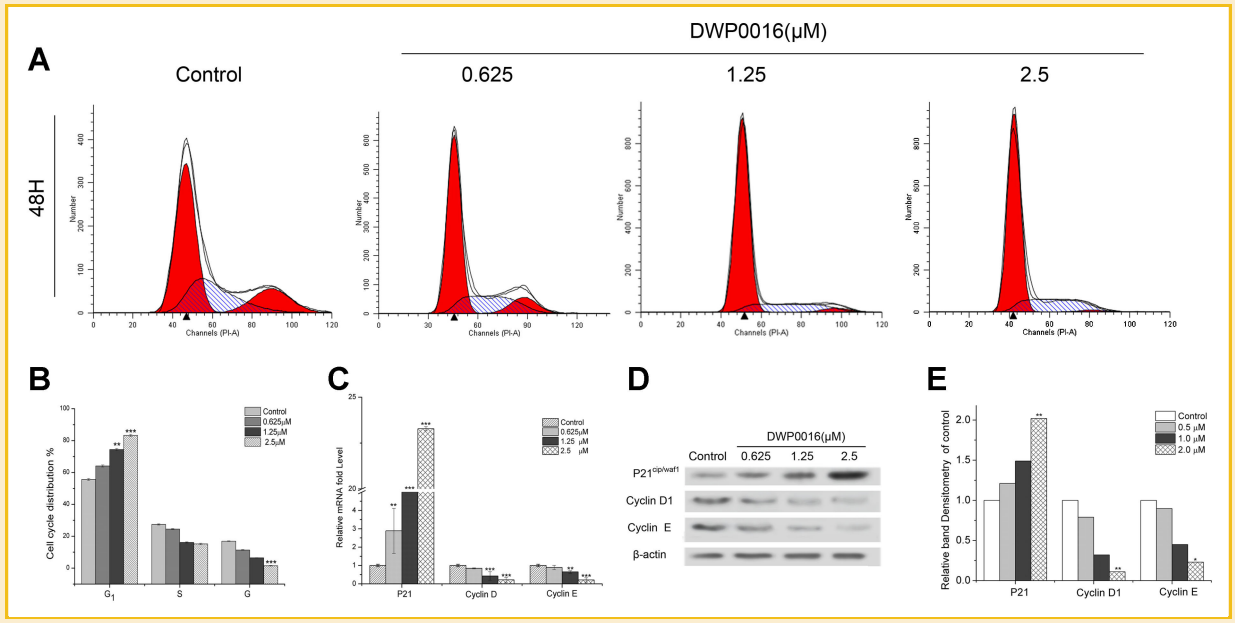

Fig. 4. A: Cell cycle distributions in U251 cells with DWP0016 treatment in different concentrations as indicated. B: The analysis of cell cycle distributions in U251 cells with DWP0016. C: Relative mRNA level regulation of p21, cyclin D, and cyclin E in U251 cells with DWP0016 treatment. The columns represented mRNA fold levels with DWP0016 at concentrations as indicated compared to the control. D: Protein expression of p21, cyclin D, and cyclin E in U251 cells with DWP0016 treatment. E: Densitometry analyzed on density of the bands. Cells were incubated with by DWP0016 in concentration as indicated for 48 h before performing the experiments. All data were expressed as means ± SD of three separate experiments. Significantly differences from control were indicated as $^{*}P < 0.05$; $^{**}P < 0.01$; $^{***}P < 0.001$.

regulation on caspase-3. DWP0016 did not affect the activity of caspase-8 as no statistical significance between the treated versus the control ($P > 0.05$). Besides, the protein expression of caspase-specific degradation of PARP was up-regulated dose-dependently in U251 cells with DWP0016, which intensively confirmed the activation of caspase-3 (Fig. 5F).

Then we used caspases inhibitor Z-VAD to investigate whether the apoptosis was caspases-dependent. The Western blotting results shown in Figure 5G confirmed the inhibition on caspases with Z-VAD. The data in Figure 5H showed that the total percentage of apoptotic cells was 4.52% with Z-VAD treatment in the concentration as indicated, which made no statistical significance versus the control (3.87%; $P > 0.05$). The apoptosis proportion was 53.45% in DWP0016 treated U251 cells. The apoptosis proportion was 42.57% in DWP0016 plus Z-VAD treated U251 cells, which still made statistical significance versus the control ($P < 0.05$). Additionally, the growth inhibition caused by DWP0016 was not sufficiently blocked with Z-VAD in U251 cells (Fig. 5I). The results are suggestible that the apoptosis was partially dependent on caspases activation. These data suggested that other caspases independent mechanisms involved in the apoptosis facilitating the growth inhibition.

DWP0016 RECRUITED P300, CBP, AND PCAF TO ACTIVATE P53 AND ACETYLATED P53 AT *LYS*382 IN U251 CELLS

We examined the mRNA level and protein expression of p53 in DWP0016-treated U251 cells. As shown in Figure 6A, the mRNA level of p53 elevated dose-dependently as the concentrations increased. At the concentration of 0.3125 μM with DWP0016, the level was 4.03-fold of the control. When the concentrations rose to 0.625 and 1.25 μM, the mRNA level were correspondingly promoted to 14.74-fold and 24.58-fold. The mRNA level in U-87 cells did not elevate with DWP0016 (Fig. 6A). Further investigations showed the protein expression of p53 was also up-regulated dose-dependently in U251 cells with DWP0016 (Fig. 6B). We detected the expression of p53 acetyl-modification with DWP0016 by using an anti-acetyl-p53 (*lys*382) antibody. As shown in Figure 6B, DWP0016 induced an ascendant expression of acetylated-p53 (*lys*382) dose-dependently in U251 cells. SAHA did not affect the acetylation of p53 in U251 cells. Neither the protein level of p53 nor acetyl-p53 was observed in U-87 cells with DWP0016 (Fig. 6B). The densitometry result was consistently with the protein expression results in the cells (Fig. 6C). To explore the mechanism of p53 acetylation, a Co-IP assay was performed to test the interaction of co-activators (PCAF and p300/CBP, with activity of histone acetylates) and p53 in U251 cells. As shown in Figure 6D and E, DWP0016 induced recruitment of p300, CBP and PCAF to interact with p53 in a dose-dependent manner. These results indicated that DWP0016 activated the transcription and expression of p53, promoted the acetylation of p53 at lys382. The activation of p53 related to the up-regulation on co-activators PCAF and p300/CBP.

DWP0016 PROMOTED PUMA TO TRIGGER BCL-2 MITOCHONDRIA APOPTOSIS PATHWAY

We examined the protein expression of PUMA, which could be direct transcriptional stimulated by p53. As indicated in Figure 6F, the

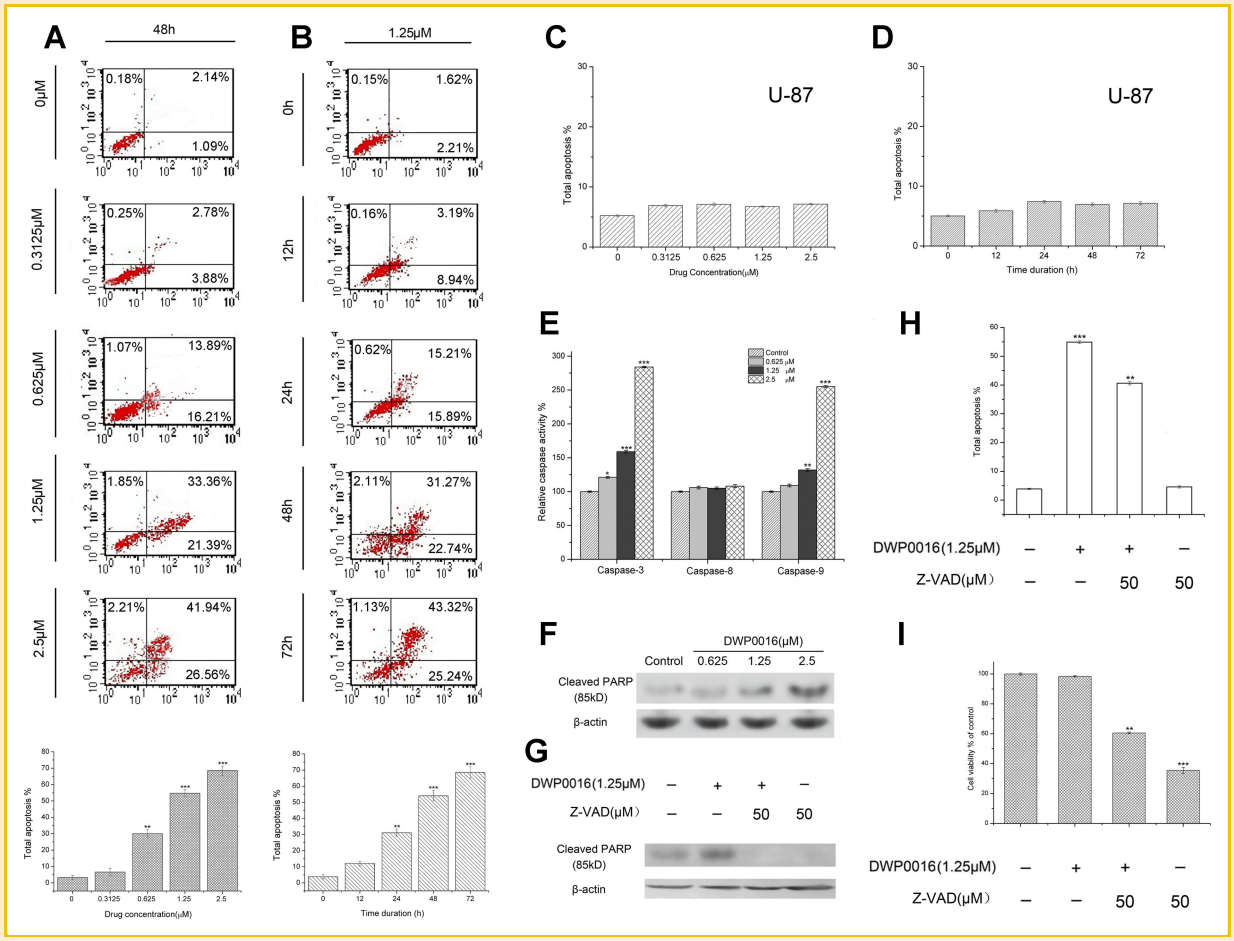

Fig. 5. A. Induction of apoptosis in U251 cells with DWP0016 treatment at different concentrations as indicated. U251 cells were treated with DWP0016 for 48 h before stained by Annexin V-FITC/PI and flow cytometric analysis. B: Induction of apoptosis in U251 cells with DWP0016 for different time duration. C: Induction of apoptosis in U-87 cells with DWP0016 treatment in different concentrations as indicated for 48 h. D: Induction of apoptosis in U251 cells with DWP0016 for different time duration. E: Relative activity of caspases activity. F: Induction of cleaved PARP in U251 cells with DWP0016 treatment in different concentrations as indicated. G: The effects of cleaved PARP induction in U251 cells with caspase inhibitor Z-VAD treatment. H: Induction of apoptosis in U251 cells with DWP0016 and/or Z-VAD treatment. I: The growth of U251 cells by DWP0016 and/or Z-VAD treatment. All data were expressed as means ± SD of three separate experiments. Significantly differences from control were indicated as $^{*}P < 0.05$; $^{**}P < 0.01$; $^{***}P < 0.001$.

protein expression of PUMA was also up-regulated by DWP0016 in a dose-dependent manner because of p53 activation. As p53 activation could catalyze Bcl-2 mitochondria apoptosis pathway, we then detected the protein expression of Bcl-2, Bax, and Bid in U251 cells. As shown in Figure 6F, the expressions of anti-apoptotic gene Bcl-2 down-regulated with DWP0016 dose-dependently. As for pro-apoptotic genes Bax and Bid, the expressions up-regulated with DWP0016 both dose-dependently. Then we examined expression of cytochrome C in cytoplasm from DWP0016-treated U251 cells. As shown in Figure 6F, the protein expression of cytochrome C up-regulated with DWP0016. The densitometry results displayed in Figure 6G was also consistent with the protein expression results. These observations made sense that after p53 activation by DWP0016, PUMA was directly stimulated and became a crucial scaffold for triggering mitochondria pathway. Then DWP0016 regulated Bcl-2, Bax, and Bid to released cytochrome C and finally induced apoptosis in U251 cells.

P53 SILENCING BLOCKED THE CELL GROWTH INHIBITION, CYCLE ARREST, AND APOPTOSIS INDUCED BY DWP0016 IN U251 CELLS

We used a specific p53 silencing siRNA assay to assess the role of p53 playing in DWP0016-induced cell growth inhibition, cell cycle arrest, and apoptosis. We found the cell growth inhibition, cell cycle arrest, and apoptosis were sufficiently blocked in U251 cells with DWP0016 after p53 silencing. As shown in Figure 7A, the expression of p53, p21, and PUMA were negative in U251 cells with p53 siRNA. The cell viability in p53 silenced U251 cells was 96.17% with DWP0016 treatment, which made no statistical difference to the untreated ($P > 0.05$; Fig. 7B). Besides, the total apoptosis was 6.17% with DWP0016 plus p53 siRNA whereas the value was 50.52% ($P < 0.001$) without siRNA (Fig. 7C). Additionally, the G_1 phase arrest was reversed with DWP0016 plus p53 siRNA treatment (Fig. 7D). These findings suggested that knockdown of p53 sufficiently blocked the cell growth inhibition, cycle arrest, and apoptosis induced by DWP0016 treatment. These results confirmed

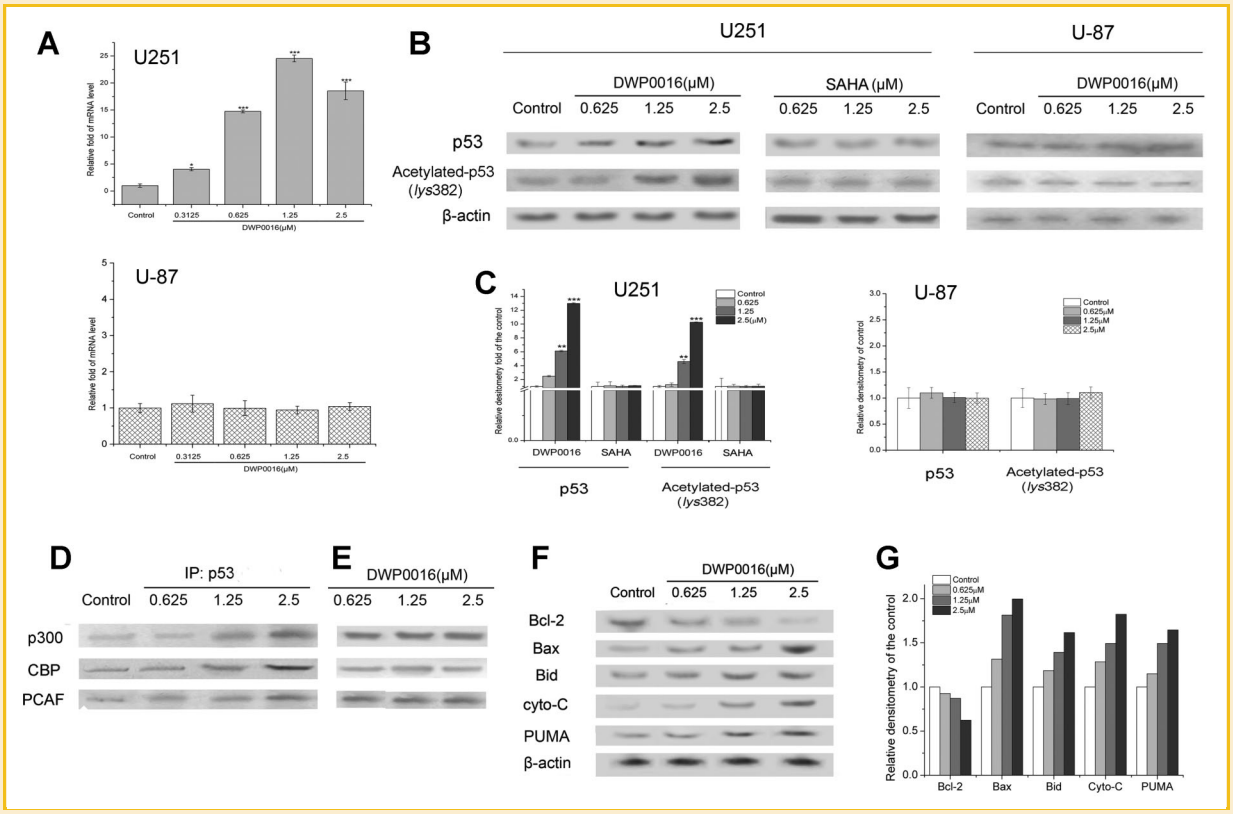

Fig. 6. A: Relative mRNA level of p53 in DWP0016 treated U251 and U-87 cells. Cells were incubated with DWP0016 at concentration as indicated for 48 h before performing real-time PCR. B: Protein expression of p53, acetyl-p53(*lys382*) in U251 and U-87 cells with DWP0016 or SAHA treatment. C: Densitometry analyzed on density of the bands. D: Co-IP protein expression with anti-p300, anti-CBP, and anti-PCAF by Western blotting with anti-p53. Cells were incubated with DWP0016 in indicated concentration for 48 h before cell protein were extracted and analyzed by Western blotting. E: Protein expression of p300, CBP, and PCAF in DWP0016 treated U251 cells. Western blots results was produced by reprobing with the same anti-p300, anti-CBP, and anti-PCAF as those used for determining IP efficiency. F: Bcl-2, Bax, Bid, cyto-C, and PUMA in U251 cells with DWP0016 exposure. G: Densitometry analyzed on density of the bands. Cells were incubated with DWP0016 in indicated concentration for 48 h before extracted and WB performed. All data were expressed as means ± SD of three separate experiments. Significantly differences from control were indicated as $^{*}P < 0.05$; $^{**}P < 0.01$; $^{***}P < 0.001$.

that p53 was a target gene of DWP0016 and responsible for the cell anti-tumor effects of DWP0016 in U251 cells.

DISCUSSION

HDAC inhibitors are recognized as effective new therapies in preclinical and clinical trials for several diseases especially for cancer. New, effective, and safe HDAC inhibitors are still in demand especially for certain cancer. Although different HDACi with mechanisms researches are reported to treat glioblastoma, the applications to treat glioblastoma with HDACi remained largely unknown. In this study, we report DWP0016 effectively inhibited U251 glioblastoma cells but not affected human astrocytes. DWP0016 activated transcription and acetylation of p53 to induce cell cycle and apoptosis in U251 glioblastoma cells. Our studies suggest post-transcriptional activation of p53 is potential for glioblastoma treatment with HDACi such as DWP0016.

U251 cell line comes from glioblastoma, which is a malignant astrocytic glioma. Malignant astrocytic glioma such as glioblastoma are the most common and lethal intracranial tumors. These cancers exhibit a relentless malignant progression characterized by widespread invasion throughout the brain, resistance to traditional therapeutic approaches, destruction of normal brain tissue, and certain death [Furnari et al., 2007]. Guided by the verifications of HDACi, we found DWP0016 induced effective growth inhibition in five carcinoma cell lines especially in U251 and U87 glioblastoma cell lines (Fig. 2A–D,G). Importantly, DWP0016 did not affect the proliferation of normal cell line L-02 nor the HA—from the same lineage of glioblastoma (Fig. 2E,F). Some documents report that specifically targeting the isoform(s) contributed to better anti-tumor performance and lower toxicity of HDACi [Balasubramanian et al., 2009]. Among the isoforms, HDAC-1 is especially essential for proliferation of human cancer cells [Lagger et al., 2002; Senese et al., 2007]. The prominent antitumor activity with fewer side effects of DWP0016 possibly attributes to the inhibition on HDAC-1. Besides, according to structure analysis, there is a 5-hydroxytryptamine (5-HT) group in DWP0016. 5-HT or Serotonin is a monoamine neurotransmitter, which interacts with 5-HT receptors and plays very important roles the central and peripheral nervous systems [Hoyer et al., 1994; Hoyer et al., 2002; Svejda et al., 2010]. The structural similarity is another bonus for DWP0016 to exhibit

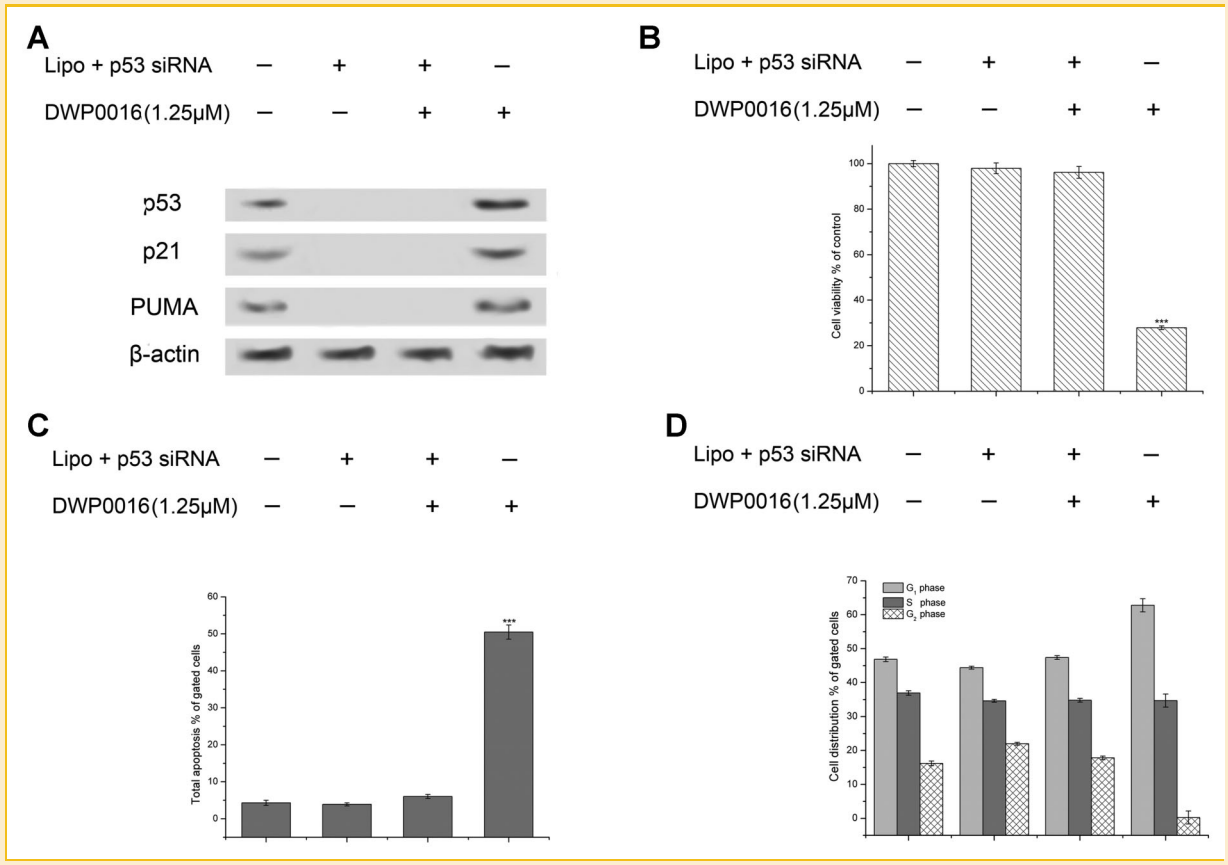

Fig. 7. P53 silencing effects in U251 cells with DWP0016. A: The expression of p53, p21, and PUMA with DWP0016 as indicated. B: Growth inhibition blocks in p53 silencing or not U251 cells with DWP0016. C: Total apoptosis percentage induction inhibition blocks of U251 cells. D: Cell cycle arrest inhibition blocks of U251 cells. For siRNA assay, cells were incubated with siRNA with treatment as indicated before MTT assay, flowcytometry analysis, and Western blotting. All experiments in vitro were performed at least thrice and independently. Significant differences from untreated control were indicated as $^{*}P < 0.05$; $^{**}P < 0.01$; $^{***}P < 0.001$.

especially effective anti-tumor efficacy in glioblastoma. However, other isoforms might involve in the effects of DWP0016. Besides, whether DWP0016 could across the blood brain barrier or not remains unknown. These hypotheses need further investigations and the explorations are on our agenda.

The cell cycle arrest effects and the apoptosis induction with DWP0016 were found consistently with other reports on HDACi [Hamada et al., 2005]. One of the cell cycle arrest and apoptosis induction mechanisms underlying the effects of HDACi is believed that inhibition of histone deacetylation may activate inappropriately silenced genes such as $p21^{waf/cip}$ [Edwards et al., 2005]. However, the induction of $p21^{WAF1}$ is not essentially required for HDAC inhibitor-induced apoptosis [Marks et al., 2001, 2003b]. Aimed to find out the key regulator of DWP0016, we focus on another important tumor suppressor p53, which is important for glioma treatment and commonly regulated by HDAC inhibitors [Drummond et al., 2005; Yang and Seto, 2007]. As previously reported, p53 coordinates cell-cycle progression and apoptosis through both transcription-dependent and post-translation-dependent mechanisms [Vousden and Lane, 2007]. Post-translational modification of p53 has critical effects on its stability and function, including phosphorylation, acetylation, sumoylation, neddylation, and methylation [Kruse and Gu, 2009]. Acetylation is one important modified form for p53 to function as a suppressor. Acetylation of p53 lead to p53 protein accumulations, which is indispensible for p53 activation [Tang et al., 2008]. HDAC inhibitors have the ability to induce p53 acetylation at lysine resulting in progression of the cell cycle arrest and apoptotic cell death. In this study, we focally detected the transcription and post-transcription on p53 in U251 cells with DWP0016. We found DWP0016 up-regulated the mRNA level and the protein expression of p53 dose-dependently. Besides, an ascendant expression of acetylated-p53 (*lys*382) in a dose-dependent manner was observed in DWP0016 but not SAHA treated cells (Fig. 6A,B). The expression of p300, CBP, and PCAF was up-regulated by DWP0016 in a dose-dependent manner, which indicated DWP0016 augmented the interaction between p300/CBP and PCAF. As p53 recruited p300/CBP and PCAF to induce p53 acetylation (Fig. 6D,E). It is reasonable to believe that up regulation on p300/CBP and PCAF led to the p53 acetylation induced by DWP0016. In other words, DWP0016 up-regulated the transcriptional and acetylation of p53 to cause p53 activation in U251 cells. Up to now to our best knowledge, there is only TSA and Depsipeptides, which are able to induce acetylation of p53 [Park et al., 2006; Zhao et al., 2006]. The acetylation of p53 with DWP0016

highlights the anti-glioblastoma potential of DWP0016. These founding also suggests that acetylation modification of p53 is potential to treat glioblastoma.

As previously reported, U251 cell line is p53 mutant and U-87 cell line is p53 wild-type [Siegelin et al., 2010; Koul et al., 2012]. We compared the p53 regulations in U251 cells to those in U-87 cells. Interestingly, although DWP0016 inhibited the growth of U-87 glioblastoma cells, DWP0016 did not induced apoptosis in U-87 cells (Fig. 5C,D). Further investigations showed DWP0016 did not affect the mRNA level nor the protein expression of p53 or acetyl-p53 in U-87 cell (Fig. 6A,B). Previous studies show U87 cell line exhibits significant dissimilarities when compared with the U251 cell line [Camphausen et al., 2005; Candolfi et al., 2007; Radaelli et al., 2009]. One of the possible explanations is that the difference is due to the different gene profiles of U87 and U251 cells [Camphausen et al., 2005]. Besides, other regulators such as PTEN [Lee et al., 2010], WOX1 [Chiang et al., 2012], and ZEB2 [Qi et al., 2012] may play a much more important role to induce cytotoxicity depending on the cell types. The reason why DWP0016 showed different effects in U87 cells may be due to genotype diversity or other involving regulators. Interestingly, a recent study on another HDAC inhibitor TSA reported the same phenomenon between cell lines harboring different status of p53. In that paper, TSA did not induce apoptosis in p53 wild-type U-87 cells, but induce apoptosis in p53 mutant U138 glioblastoma cells [Bajbouj et al., 2012]. In consideration of the facts that DWP0016 and TSA are both hydroximic acid homologues, it is rational to believe the difference between U251 and U-87 cells is due to the diversity of cell lines.

Activation of p53 triggered mitochondrial pathway to induce apoptosis via PUMA stimulation, which was correlative to the Bcl-2 family [Miyashita and Reed, 1995; Nakano and Vousden, 2001; Jeffers et al., 2003; Hastak et al., 2005]. We found DWP0016 PUMA was up-regulated as a result of P53 activation. Up regulation of PUMA scaffolded to trigger mitochondria pathway. Then DWP0016 regulated Bcl-2, Bax, and Bid to released cytochrome C and finally induced apoptosis in U251 cells. These results were consistent with the descriptions in other documents [Yu and Zhang, 2008]. To identify the role of p53 in the effects of DWP0016-treated U251 cells, the siRNA technique was used to selectively knockdown the p53 gene. We found the p53 silencing by transient transfection with siRNA resulted in sufficient block on cell growth inhibition, cell cycle arrest, and apoptosis (Fig. 7A–D). These results indicated that P53 was a key target of DWP0016 involved in the molecular mechanisms and played a much more dominant role beyond other regulators.

A high percentage of human tumors maintain overexpression of various mutant forms of p53 [Hussain and Harris, 1998]. The majority of the p53 mutations are missense mutations, leading to the expression of the full-length p53 mutants with incapacity of activating p53 target genes and suppressing tumorigenesis [Lu et al., 2012]. Some mutant p53 forms acquire new oncogenic properties which are known as ''gain-of-function'' properties [Dittmer et al., 1993]. These mutant p53 transcriptionally regulate genes that mediate proliferation, drug-resistance, survival, metastasis, etc. [Brosh and Rotter, 2009]. Different reports show mutant p53 transactivated viral and cellular promoters including the MDR-1 [Lin et al., 1995], c-myc [Frazier et al., 1998], etc. In glioma cells, mutant p53 status has been reported to be an unfavorable factor for radiotherapy effectiveness and poor prognosis [Squatrito et al., 2010]. In our study, DWP0016 induced caspase and mitochondrial apoptosis in U251 cells. The effects in U251 cells consistent with that induced by the p53-mediated apoptosis in glioma cells [Shinoura et al., 1999]. As DWP0016 is able to acetylate p53, one of the possible explanations is that acetylation of p53 with DWP0016 restore at least part of p53 function in U251 cells. Clearly, this is speculation and need more investigations. Anyway, DWP0016 acetylated p53 to inhibit the proliferation in U251 cells, which may shed a light for the further development of preferentially therapy for mutant p53 cancers.

In summary, we find HDAC inhibitor DWP0016 is a promising anticancer therapeutic candidate for glioblastoma treatment with its intended p53 activation mechanism. DWP0016 induced p53 acetylation at lys382, which benefited from the up-regulation of co-activators p300, CBP, and PCAF. Furthermore, our reports suggest that the post-modification to activate p53 with inhibiting HDAC activity was potent and practical to treat glioblastoma.

ACKNOWLEDGMENTS

This work is supported by the Shanghai Committee of Science and Technology (09JC1404500, 10JC1414500); Shanghai Leading Academic Discipline Project, Project No. B507. The authors are grateful to all of the colleagues for their valuable discussion during the preparation of this manuscript.

REFERENCES

Acharya M, Sparreboom A, Venitz J, Figg W. 2005. Rational development of histone deacetylase inhibitors as anticancer agents: a review. Mol Pharmacol 68:917.

Adams J, Cory S. 2007. The Bcl-2 apoptotic switch in cancer development and therapy. Oncogene 26:1324.

Bajbouj K, Mawrin C, Hartig R, Schulze-Luehrmann J, Wilisch-Neumann A, Roessner A, Schneider-Stock R. 2012. P53-dependent antiproliferative and pro-apoptotic effects of trichostatin A (TSA) in glioblastoma cells. J Neurooncol 107(3):503–516.

Balasubramanian S, Verner E, Buggy JJ. 2009. Isoform-specific histone deacetylase inhibitors: The next step? Cancer Lett 280:211–221.

Baylin S, Ohm J. 2006. Epigenetic gene silencing in cancer—A mechanism for early oncogenic pathway addiction? Nat Rev Cancer 6:107–116.

Bolden J, Peart M, Johnstone R. 2006. Anticancer activities of histone deacetylase inhibitors. Nat Rev Drug Discov 5:769–784.

Brosh R, Rotter V. 2009. When mutants gain new powers: News from the mutant p53 field. Nat Rev Cancer. 9(10):701–713.

Camphausen K, Purow B, Sproull M, Scott T, Ozawa T, Deen DF, Tofilon PJ. 2005. Influence of in vivo growth on human glioma cell line gene expression: Convergent profiles under orthotopic conditions. Proc Natl Acad Sci USA 102:8287–8292.

Candolfi M, Curtin JF, Nichols WS, Muhammad AKMG, King GD, Pluhar GE, McNiel EA, Ohlfest JR, Freese AB, Moore PF. 2007. Intracranial glioblastoma models in preclinical neuro-oncology: Neuropathological characterization and tumor progression. J Neurooncol 85:133–148.

Chen C, Weng S, Tseng P, Lin H. 2005. Histone acetylation-independent effect of histone deacetylase inhibitors on Akt through the reshuffling of protein phosphatase 1 complexes. J Biol Chem 280:38879.

Chiang M-F, Yeh S-T, Liao H-F, Chang N-S, Chen Y-J. 2012. Overexpression of WW domain-containing oxidoreductase WOX1 preferentially induces apoptosis in human glioblastoma cells harboring mutant p53. Biomed Pharmacother 66:433–438.

Choudhary C, Kumar C, Gnad F, Nielsen M, Rehman M, Walther T, Olsen J, Mann M. 2009. Lysine acetylation targets protein complexes and co-regulates major cellular functions. Science 14;325(5942):834–840.

Dittmer D, Pati S, Zambetti G, Chu S, Teresky AK, Moore M, Finlay C, Levine AJ. 1993. Gain of function mutations in p53. Nat Genet 4:42–46.

Drummond D, Noble C, Kirpotin D, Guo Z, Scott G, Benz C. 2005. Clinical development of histone deacetylase inhibitors as anticancer agents. Pharmacol Toxicol 45:495.

Edwards L, Thiessen B, Dragowska W, Daynard T, Bally M, Dedhar S. 2005. Inhibition of ILK in PTEN-mutant human glioblastomas inhibits PKB/Akt activation, induces apoptosis, and delays tumor growth. Oncogene 24:3596–3605.

Egger G, Liang G, Aparicio A, Jones P. 2004. Epigenetics in human disease and prospects for epigenetic therapy. Nature 429:457–463.

Eyülpoglu IY, Hahnen E, Buslei R, Siebzehnrülbl FA, Savaskan NE, Lülders M, Trnkle C, Wick W, Weller M, Fahlbusch R. 2005. Suberoylanilide hydroxamic acid (SAHA) has potent anti-glioma properties in vitro, ex vivo and in vivo. J Neurochem 93(4):992–999.

Fournel M, Bonfils C, Hou Y, Yan P, Trachy-Bourget M, Kalita A, Liu J, Lu A, Zhou N, Robert M. 2008. MGCD0103, a novel isotype-selective histone deacetylase inhibitor, has broad spectrum antitumor activity in vitro and in vivo. Mol Cancer Ther 7:759.

Frazier MW, He X, Wang JL, Gu Z, Cleveland JL, Zambetti GP. 1998. Activation of c-myc gene expression by tumor-derived p53 mutants requires a discrete C-terminal domain. Mol Cell Biol 18:3735–3743.

Furnari FB, Fenton T, Bachoo RM, Mukasa A, Stommel JM, Stegh A, Hahn WC, Ligon KL, Louis DN, Brennan C. 2007. Malignant astrocytic glioma: Genetics, biology, and paths to treatment. Genes Develop 21:2683.

Gan Y, Wang J, Coselli J, Wang X. 2008. Synergistic induction of apoptosis by HMG-CoA reductase inhibitor and histone deacetylases inhibitor in HeLa cells. Biochem Biophys Res Commun 365:386–392.

Gray S, Ekstrm T. 2001. The human histone deacetylase family. Exp Cell Res 262:75–83.

Grzmil M, Morin P, Lino MM, Merlo A, Frank S, Wang Y, Moncayo G, Hemmings BA. 2011. MAP kinase-interacting kinase 1 regulates SMAD2-dependent TGF-β signaling pathway in human glioblastoma. Cancer Res 71(6):2392–2402.

Guo A, Salomoni P, Luo J, Shih A, Zhong S, Gu W, Pandolfi PP. 2000. The function of PML in p53-dependent apoptosis. Nat Cell Biol 2:730–736.

Hamada K, Sasaki T, Koni P, Natsui M, Kishimoto H, Sasaki J, Yajima N, Horie Y, Hasegawa G, Naito M. 2005. The PTEN/PI3K pathway governs normal vascular development and tumor angiogenesis. Genes Develop 19:2054.

Hastak K, Agarwal MK, Mukhtar H, Agarwal ML. 2005. Ablation of either p21 or Bax prevents p53-dependent apoptosis induced by green tea polyphenol epigallocatechin-3-gallate. FASEB J 19:789.

Hoyer D, Clarke DE, Fozard JR, Hartig P, Martin GR, Mylecharane EJ, Saxena PR, Humphrey P. 1994. International Union of Pharmacology classification of receptors for 5-hydroxytryptamine (Serotonin). Pharmacol Rev 46:157–203.

Hoyer D, Hannon JP, Martin GR. 2002. Molecular, pharmacological and functional diversity of 5-HT receptors. Pharmacol Biochem Behav 71:533–554.

Hussain SP, Harris CC. 1998. Molecular epidemiology of human cancer: Contribution of mutation spectra studies of tumor suppressor genes. Cancer Res 58(18):4023–4037.

Ito A, Lai CH, Zhao X, Saito S, Hamilton MH, Appella E, Yao TP. 2001. p300/CBP-mediated p53 acetylation is commonly induced by p53-activating agents and inhibited by MDM2. EMBO J 20:1331–1340.

Jeffers JR, Parganas E, Lee Y, Yang C, Wang JL, Brennan J, MacLean KH, Han J, Chittenden T, Ihle JN. 2003. Puma is an essential mediator of p53-dependent and-independent apoptotic pathways. Cancer Cell 4:321–328.

Koul D, Fu J, Shen R, LaFortune TA, Wang S, Tiao N, Kim YW, Liu JL, Ramnarian D, Yuan Y. 2012. Antitumor activity of NVP-BKM120—A selective pan class I PI3 kinase inhibitor showed differential forms of cell death based on p53 status of glioma cells. Clin Cancer Res 18:184–195.

Kruse JP, Gu W. 2009. Modes of p53 regulation. Cell 137:609–622.

Kumagai T, Wakimoto N, Yin D, Gery S, Kawamata N, Takai N, Komatsu N, Chumakov A, Imai Y, Koeffler HP. 2007. Histone deacetylase inhibitor, suberoylanilide hydroxamic acid (Vorinostat, SAHA) profoundly inhibits the growth of human pancreatic cancer cells. Int J Cancer 121:656–665.

Lagger G, O'Carroll D, Rembold M, Khier H, Tischler J, Weitzer G, Schuettengruber B, Hauser C, Brunmeir R, Jenuwein T. 2002. Essential function of histone deacetylase 1 in proliferation control and CDK inhibitor repression. EMBO J 21:2672–2681.

Lee JJ, Kim BC, Park MJ, Lee YS, Kim YN, Lee BL, Lee JS. 2010. PTEN status switches cell fate between premature senescence and apoptosis in glioma exposed to ionizing radiation. Cell Death Differ 18:666–677.

Li Y, Mao Y, Brandt-Rauf P, Williams A, Fine R. 2005. Selective induction of apoptosis in mutant p53 premalignant and malignant cancer cells by PRIMA-1 through the c-Jun-NH2-kinase pathway. Mol Cancer Ther 4:901.

Liang X, Xu Y, Xu K, Liu J, Qian X. 2010. B1, a novel amonafide analogue, overcomes the resistance conferred by Bcl-2 in human promyelocytic leukemia HL60 cells. Mol Cancer Res 8:1619.

Lin J, Teresky AK, Levine AJ. 1995. Two critical hydrophobic amino acids in the N-terminal domain of the p53 protein are required for the gain of function phenotypes of human p53 mutants. Oncogene 10:2387.

Liu Y, Zhang S, Cai Y. 2007. Cytoprotective effects of selenium on cadmium-induced LLC-PK1 cells apoptosis by activating JNK pathway. Toxicol In Vitro 21:677–684.

Lu X, Liu DP, Xu Y. 2012. The gain of function of p53 cancer mutant in promoting mammary tumorigenesis. Oncogene. DOI: 10.1038/onc.2012.299 [Epub ahead of print].

Luo J, Su F, Chen D, Shiloh A, Gu W. 2000. Deacetylation of p53 modulates its effect on cell growth and apoptosis. Nature 408:377–381.

Marks PA, Rifkind RA, Richon VM, Breslow R, Miller T, Kelly WK. 2001. Histone deacetylases and cancer: Causes and therapies. Nat Rev Cancer 1:194–202.

Marks P, Miller T, Richon V. 2003a. Histone deacetylases. Curr Opin Pharmacol 3:344–351.

Marks PA, Miller T, Richon VM. 2003b. Histone deacetylases. Curr Opin Pharmacol 3:344–351.

Miyashita T, Reed J. 1995. Tumor suppressor p53 is a direct transcriptional activator of the human bax gene. Cell 80:293.

Nagarajan RP, Costello JF. 2009. Epigenetic mechanisms in glioblastoma multiformeeditor, Elsevier, 19(3):188–197.

Nakano K, Vousden KH. 2001. PUMA, a novel proapoptotic gene, is induced by p53. Mol Cell 7:683–694.

Park HY, Kim MK, Moon SI, Cho YH, Lee CH. 2006. Cell cycle arrest and apoptotic induction in LNCaP cells by MCS-C2, novel cyclin©\dependent kinase inhibitor, through p53/p21WAF1/CIP1 pathway. Cancer Sci 97:430–436.

Qi S, Song Y, Peng Y, Wang H, Long H, Yu X, Li Z, Fang L, Wu A, Luo W. 2012. ZEB2 mediates multiple pathways regulating cell proliferation, migration, invasion, and apoptosis in glioma. PLoS ONE 7:e38842.

Radaelli E, Ceruti R, Patton V, Russo M, Degrassi A, Croci V, Caprera F, Stortini G, Scanziani E, Pesenti E. 2009. Immunohistopathological and

neuroimaging characterization of murine orthotopic xenograft models of glioblastoma multiforme recapitulating the most salient features of human disease. Histol Histopathol 24:879.

Senese S, Zaragoza K, Minardi S, Muradore I, Ronzoni S, Passafaro A, Bernard L, Draetta G, Alcalay M, Seiser C. 2007. Role for histone deacetylase 1 in human tumor cell proliferation. Mol Cell Biol 27:4784.

Shinoura N, Muramatsu Y, Nishimura M, Yoshida Y, Saito A, Yokoyama T, Furukawa T, Horii A, Hashimoto M, Asai A. 1999. Adenovirus-mediated transfer of p33ING1 with p53 drastically augments apoptosis in gliomas. Cancer Res 59:5521–5528.

Siegelin MD, Raskett CM, Gilbert CA, Ross AH, Altieri DC. 2010. Sorafenib exerts anti-glioma activity in vitro and in vivo. Neurosci Lett 478:165–170.

Squatrito M, Brennan CW, Helmy K, Huse JT, Petrini JH, Holland EC. 2010. Loss of ATM/Chk2/p53 pathway components accelerates tumor development and contributes to radiation resistance in gliomas. Cancer Cell 18: 619–629.

Stambolic V, MacPherson D, Sas D, Lin Y, Snow B, Jang Y, Benchimol S, Mak T. 2001. Regulation of PTEN transcription by p53. Mol Cell 8:317–325.

Stegh AH, DePinho RA. 2011. Beyond effector caspase inhibition: Bcl2L12 neutralizes p53 signaling in glioblastoma. Cell cycle (Georgetown, Tex.) 10.

Svejda B, Kidd M, Giovinazzo F, Eltawil K, Gustafsson BI, Pfragner R, Modlin IM. 2010. The 5-HT2B receptor plays a key regulatory role in both neuroendocrine tumor cell proliferation and the modulation of the fibroblast component of the neoplastic microenvironment. Cancer 116:2902–2912.

Tang Y, Zhao W, Chen Y, Zhao Y, Gu W. 2008. Acetylation is indispensable for p53 activation. Cell 133:612–626.

Ugur HC, Ramakrishna N, Bello L, Menon LG, Kim SK, Black PM, Carroll RS. 2007. Continuous intracranial administration of suberoylanilide hydroxamic acid (SAHA) inhibits tumor growth in an orthotopic glioma model. J Neurooncol 83:267–275.

Vousden KH, Lane DP. 2007. p53 in health and disease. Nat Rev Mol Cell Biol 8:275–283.

Watanabe K, Sato K, Biernat W, Tachibana O, von Ammon K, Ogata N, Yonekawa Y, Kleihues P, Ohgaki H. 1997. Incidence and timing of p53 mutations during astrocytoma progression in patients with multiple biopsies. Clin Cancer Res 3:523.

Yang X, Seto E. 2007. HATs and HDACs: From structure, function and regulation to novel strategies for therapy and prevention. Oncogene 26:5310–5318.

Yu J, Zhang L. 2008. PUMA, a potent killer with or without p53. Oncogene 27:S71–S83.

Zhao Y, Lu S, Wu L, Chai G, Wang H, Chen Y, Sun J, Yu Y, Zhou W, Zheng Q. 2006. Acetylation of p53 at lysine 373/382 by the histone deacetylase inhibitor depsipeptide induces expression of p21Waf1/Cip1. Mol Cell Biol 26:2782.

Zhu WG, Lakshmanan RR, Beal MD, Otterson GA. 2001. DNA methyltransferase inhibition enhances apoptosis induced by histone deacetylase inhibitors. Cancer Res 61:1327.